JACS
JOURNAL OF THE AMERICAN CHEMICAL SOCIETY

Communication

pubs.acs.org/JACS

Observation of Single-Protein and DNA Macromolecule Collisions on Ultramicroelectrodes

Jeffrey E. Dick, Christophe Renault, and Allen J. Bard*

Center for Electrochemistry, Department of Chemistry, The University of Texas at Austin, Austin, Texas 78712, United States

Supporting Information

ABSTRACT: Single-molecule detection is the ultimate sensitivity in analytical chemistry and has been largely unavailable in electrochemical analysis. Here, we demonstrate the feasibility of detecting electrochemically inactive single biomacromolecules, such as enzymes, antibodies, and DNA, by blocking a solution redox reaction when molecules adsorb and block electrode sites. By oxidizing a large concentration of potassium ferrocyanide on an ultramicroelectrode (UME, radius ≤150 nm), time-resolved, discrete adsorption events of antibodies, enzymes, DNA, and polystyrene nanospheres can be differentiated from the background by their "footprint". Further, by assuming that the mass transport of proteins to the electrode surface is controlled mainly by diffusion, a size estimate using the Stokes−Einstein relationship shows good agreement of electrochemical data with known protein sizes.

Single-molecule detection provides the ultimate sensitivity in analytical determinations and has been a subject of intense interest in electrochemistry.[1−6] Different optical methods, e.g., fluorescence and Raman spectroscopy, have been developed to monitor single-molecule processes and the electrochemistry of isolated and immobilized molecules,[7,8] but they do not provide information on molecule size or shape. Methods involving biological and solid-state nanopores have also been developed to probe the shape, size and conformation of single molecules as they pass through nanopores by resistive pulse measurements.[9] Since the first report by Lemay and co-workers, of discrete adsorption events of 1 μm diameter latex microspheres on ultramicroelectrodes (UMEs) and 25 nm CdSe nanospheres on lithographically fabricated nanoelectrodes a decade ago,[10] the observation of collisions on UMEs has received considerable attention.[11] Here, we present a method for observing electrochemically inactive single molecules using the electrochemical collision methodology. We were able to see discrete collisions of plasmid DNA (pDNA), horseradish peroxidase (HRP), glucose oxidase (GOx), mouse monoclonal antibody (IgG), and catalase (CAT) on the surface of a Pt UME. The radius of the UME (r_{UME}) is comprised between 80 and 150 nm. These collisions were marked by irreversible adsorption of the protein or DNA strand onto the electrode surface. Ultimately, the proposed methodology is the simplest technology developed to study interactions at the single-molecule level. This is the first report of single-molecule collisions on UMEs.

One way to electrochemically detect discrete collisions is shown in Figure 1. A redox molecule, like potassium ferrocyanide, is oxidized continuously at an electrode surface under diffusion-limited conditions, producing an anodic, steady-state current. Upon adsorption of an insulating object, the flux of redox-active species to the electrode is blocked, leading to a staircase-shaped decrease in steady-state current with a magnitude of Δi_{ss}. Figures 1 and 2 both display current decreases because anodic currents are plotted as negative. This means of detecting the adsorption event is termed *blocking* due

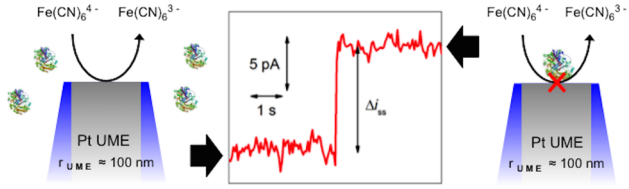

Figure 1. Schematic depiction of a blocking experiment. An insulating molecule, such as a protein, adsorbs at the surface of an UME and blocks the oxidation of ferrocyanide. Consequently, a decrease of the current (Δi_{ss}) is observed on the $i-t$ curve. The $i-t$ curve represented in the figure shows a 150 nm radius Pt UME being partially blocked by glucose oxidase.

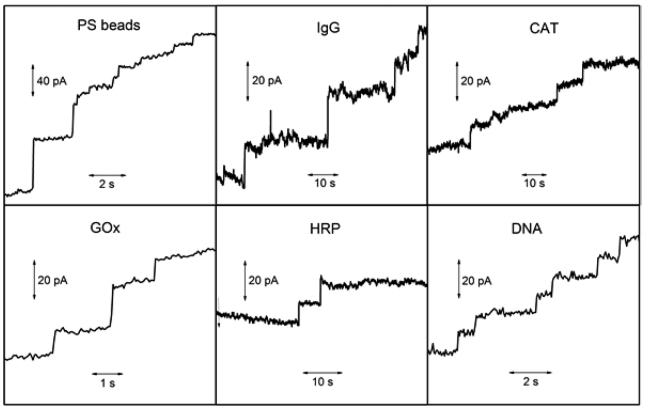

Figure 2. $i-t$ curves recorded in the presence of 7 pM polystyrene beads, 2 pM IgG, 2 pM CAT, 2 pM GOx, 2 pM HRP, and 300 pM pDNA. Pt UME biased at 0.8 V vs Ag/AgCl in a solution of 400 mM ferrocyanide was used. The sizes of the UMEs are given in Table 1. In each experiment, a data point was taken every 50 ms.

Received: May 1, 2015
Published: June 24, 2015

DOI: 10.1021/jacs.5b04545
J. Am. Chem. Soc. 2015, 137, 8376−8379

to the blocking of electrode sites. Blocking has been expanded to soft particles (i.e., emulsion droplet),[12,13] and fundamental studies on blocking have been reported.[14] An understanding of the collision footprint, i.e., the size of the current steps and the frequency with which molecules collide with the electrode, can give insight into the concentration, surface charge, and size distribution of the molecules colliding with the electrode. This blocking technique was recently used to detect single viruses, a biologically relevant analyte.[15] As a rule of thumb for observing discrete adsorption events, the radius of the adsorbate should be ca. 10% of the radius of the electrode.[14] In the reported experiments, the radius of the working electrode was between 80 and 150 nm, which would imply a detection of 8−15 nm objects. In our experiments, however, the concentration of redox-active species being blocked is 400 mM.

Several factors must be taken into account when observing and analyzing discrete collisions. First, the amount of current to be blocked has to be large enough to be distinguished from the background current as well as random fluctuations in the current due to different types of electronic noise. Second, there exists an intrinsic distribution of current step magnitudes in blocking experiments due to the so-called edge effect. Because radial diffusion on a disk UME is largest at the edges, there is a non-uniform distribution of current density on the electrode surface when faradaic current is flowing. Thus, if a molecule lands on the edge of an UME, it will block more current than a molecule of the same size and dimensions landing at the center of the electrode, resulting in a larger Δi_{ss} for the molecule landing on the edge.

Figure 2 presents $i-t$ curves obtained with sub-micrometer-sized Pt UMEs ($r_{UME} \leq 150$ nm) biased at 0.8 V vs Ag/AgCl. Details about the experimental setup are provided in the Supporting Information. The $i-t$ curves were recorded in the presence of 11 nm radius polystyrene beads (Figure 2a), four different proteins (Figure 2b−e), and a plasmid DNA (pDNA, Figure 2f). The 11 nm radius polystyrene nanospheres were used as reference particles to emphasize the possibility of seeing blocking events with rigid spheres roughly the same size as the protein molecules. The amount of current blocked is smaller than what is expected due to the spherical shape blocking the electrode, where flux around the sphere is not completely blocked due to the curvature of the bead. It should also be noted that there is an uncertainty in the protein shape in such a high concentration of ferrocyanide salt. The protein radii, measured from their crystallographic structure (found on the Protein data Bank), r_{PDB}, are provided in Table 1. The smallest protein, HRP, measures ca. 1.5 nm in radius, while the largest protein, IgG, has a radius of about 7.5 nm. The pDNA can adopt different conformations in solution, and thus its size is not well known; however, the frequency of collision can yield insight into the size and shape, *vide infra*. Several more blocking $i-t$ curve examples are provided at the end of the Supporting Information.

Table 1. Experimental Results from Electrochemical Collision Experiments

adsorbate	r_{PDB} (nm)	$r_{\Delta i}$ (nm)	r_{freq} (nm)	Δi_{ss} (pA)	r_{UME} (nm)
PSB	11 ± 1	5.9 ± 3.7	12.5 ± 3.5	30 ± 7	140
HRP	1.5	2.2 ± 1.4	3.5 ± 0.5	10 ± 2.1	100
GOx	4	6.8 ± 3.4	4.5 ± 1.5	18 ± 2.3	120
CAT	6	4.6 ± 2.5	7 ± 1	20 ± 5	80
IgG	7.5	6.5 ± 4.5	9.5 ± 2.5	15 ± 2	150

All the $i-t$ curves produce staircase-shaped current steps typical of single-particle or biomolecule collisions. Control experiments without a nanoparticle or biomolecule in solution do not show current steps. To a first approximation, the molecular size can be determined in blocking experiments from the size of the footprint (the current step magnitude, Δi_{ss}). The average current step magnitude reported in Table 1 involves the analysis of 50 or more steps and was measured over several independent experiments. The values of Δi_{ss} obtained with the polystyrene beads and the biomolecules are of the same order of magnitude (tens of pA), as expected for objects that have a size of the same order of magnitude (∼10 nm). In a previous report, we observed that Δi_{ss} is proportional to the steady-state current, i_{ss}, and the ratio of the footprint of the insulating object (of apparent radius $r_{\Delta i}$) with the electrode surface of radius r_{UME}.[14] Knowing the radius of the UME (r_{UME}, see Table 1), the change in steady-state current, and the steady-state current before the collision event, and approximating the projected contact area of the biomolecule to the area of a circle, we can derive a simple expression for the radius of the biomolecule:

$$r_{\Delta i} = r_{UME}\sqrt{\frac{\Delta i_{ss}}{i_{ss}}} \quad (1)$$

Although eq 1 does not take into account the edge effect inherent in blocking experiments on disk UMEs,[16] the shape of the object, or its permeability to ferrocyanide, it provides a simple estimate of $r_{\Delta i}$. Using eq 1 and the value of Δi_{ss} measured on the $i-t$ curves in Figure 2, we determined $r_{\Delta i}$ for the reported species. The values of $r_{\Delta i}$ are reported in Table 1. A large data spread is observed due to the various factors influencing the change in steady-state current outlined above.

Another way to estimate the size of the objects in solution is to use the frequency of collision, assuming the probability of an adsorbate sticking to the electrode is 1. The diffusive flux of biomolecules to the surface of the electrode can be represented as a frequency of collision, f_{diff}, given by the following equation:[10,17]

$$f_{diff} = 4DCr_{UME}N_A \quad (2)$$

where D is the diffusion coefficient of the molecule, C is the concentration, and N_A is Avogadro's number. From the value of D, the hydrodynamic radius of the molecule (r_h) can be determined by using the Stokes−Einstein relationship:

$$r_h = k_B T(6\pi\eta D)^{-1} \quad (3)$$

where k_B is Boltzmann's constant, T is temperature, and η is the viscosity of the solution. Hence, either the size of the protein or its concentration can be determined from the experimental frequency of collision and eqs 2 and 3, assuming that mass transfer to the UME is diffusion controlled. It is true that migration may play a role in mass transport to the electrode; however, because the medium consists of such a high concentration of potassium ferrocyanide (400 mM), migration is not the dominant source of mass transfer. From eq 2, the frequency is expected to vary linearly with concentration.

Figure 3 shows frequency versus concentration curves for each protein. From the frequency and the concentration of the protein in solution, a value of the hydrodynamic radius can be estimated using the frequency equation and Stokes−Einstein relationship. For each protein, the value of the hydrodynamic

DOI: 10.1021/jacs.5b04545
J. Am. Chem. Soc. 2015, 137, 8376−8379

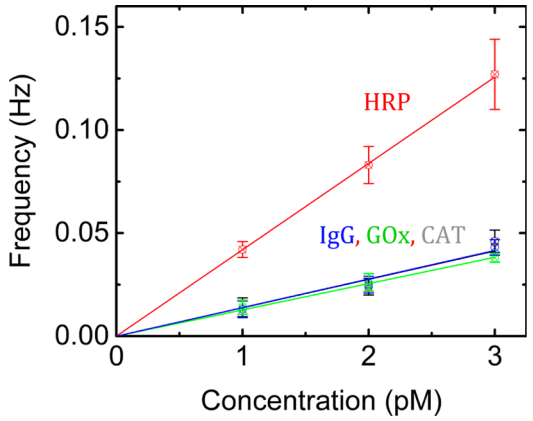

Figure 3. Frequency of current steps as a function of biomolecule concentration. The error bars correspond to the standard deviation on at least three measurements. The straight lines are linear fits of the experimental values.

radius was estimated from a linear fit of the experimental frequency shown in Figure 3 (straight line), shown in Table 1 as r_{freq}. Remarkably, the frequency analysis, based upon diffusion considerations, and the current step size analysis, based upon electrochemical considerations, independently lead to similar conclusions concerning the size of the object that is colliding with the UME. Interestingly, when acid is added in the solution of protein (initially at pH ~7 to pH ~0), the current steps are not observed (see Supporting Information, Figure S3); however, the rate of electrode deactivation is similar to that of the experiment where blocking events are observed (i.e., i–t curves are parallel). This may likely be due to denaturing of the protein upon addition of acid, and, because the protein is not as compact, discrete events are not discernible against the background. The proposed methodology can also be employed to distinguish the quality of a molecular sample, such as comparing the extent of aggregation between an old and new solution of HRP (see Supporting Information, Figure S4). A similar estimation of hydrodynamic radius can be derived from the collisional frequency of pDNA, which is composed of 1140 adenines, 1246 guanines, 1285 cytosines, and 1062 thymines. Our collision experiments suggest that pDNA has a hydrodynamic radius of about 30 nm, which could indicate a type of supercoiled conformation.

In summary, we have shown that time-resolved, discrete adsorption events of biological macromolecules can be observed on an UME, which is likely the simplest technology to date capable of single-molecule resolution. The proposed methodology yields insight into single adsorption events of molecules as opposed to ensemble molecular fouling of the electrode, and it can be used to study surface passivation by observing discrete molecule adsorption. The technique can also be useful in judging the quality and concentration of a molecular sample, allowing the use of a molecule's footprint (i.e., current step magnitude and collision frequency) to discern impurities or aggregates. The electrochemical collision methodology has pushed the limits to single-molecule detection, providing a foundation upon which single molecules can be studied as they interact with surfaces. Amplification can be gained in blocking by playing on the concentration of redox-active species being blocked, the noise level at this concentration, and the size of the adsorbing species relative to the UME. Blocking of smaller molecules should be possible with even smaller electrodes fabricated by a number of techniques, e.g., a tunneling UME,[18] which is under active investigation in our laboratory. The proposed methodology is not selective because any solution species that specifically adsorbs on the electrode will show a response. To simplify the analysis of the current step, we could envisage the fabrication and use of a hemispherical UME that displays uniform current density across the electrode surface, suppressing the edge effect, and allowing for a more direct relationship to obtain the size of individual molecules using their footprint with less ambiguity.

■ ASSOCIATED CONTENT

Supporting Information

Experimental methodology, additional experimental data, and images of UMEs. The Supporting Information is available free of charge on the ACS Publications website at DOI: 10.1021/jacs.5b04545.

■ AUTHOR INFORMATION

Corresponding Author

*ajbard@cm.utexas.edu

Notes

The authors declare no competing financial interest.

■ ACKNOWLEDGMENTS

The authors thank Dr. Jason W. Upton and Mr. Adam T. Hilterbrand for plasmid DNA and helpful discussion. J.E.D. acknowledges the National Science Foundation Graduate Research Fellowship (Grant No. DGE-1110007). We also acknowledge support of this research from the AFOSR MURI (FA9550-14-1-0003) and the Welch Foundation (F-0021). Mouse monoclonal anti-gB neutralizing antibody (Clone MAb97.3) was provided by Dr. Michael Mach (University of Erlangen, Germany), and we greatly appreciate his donation.

■ REFERENCES

(1) Bard, A. J.; Fan, F.-R. F. *Acc. Chem. Res.* **1996**, *29*, 572–578.
(2) Fan, F.-R. F.; Bard, A. J. *Proc. Natl. Acad. Sci. U.S.A.* **1999**, *96*, 14222–14227.
(3) Fan, F.-R. F.; Bard, A. J. *Science* **1995**, *267*, 871–874.
(4) Fan, F.-R. F.; Kwak, J.; Bard, A. J. *J. Am. Chem. Soc.* **1996**, *118*, 9669–9675.
(5) Zevenbergen, M. A. G.; Singh, P. S.; Goluch, E. D.; Wolfrum, B. L.; Lemay, S. G. *Nano Lett.* **2011**, *11*, 2881–2886.
(6) Sun, P.; Mirkin, M. V. *J. Am. Chem. Soc.* **2008**, *130*, 8241–8250.
(7) Palacios, R. E.; Fan, F.-R. F.; Bard, A. J.; Barbara, P. F. *J. Am. Chem. Soc.* **2006**, *128*, 9028–9029.
(8) Cortes, E.; Etchegoin, P. G.; Le Ru, E. C.; Fainstein, A.; Vela, M. E.; Salvarezza, R. C. *J. Am. Chem. Soc.* **2010**, *132*, 18034–18037.
(9) See, e.g.: Dekker, C. *Nat. Nanotechnol.* **2007**, *2*, 209–215.
(10) Quinn, B. M.; van't Hof, P. G.; Lemay, S. G. *J. Am. Chem. Soc.* **2004**, *126*, 8360–8361.
(11) Bard, A. J.; Boika, A.; Kwon, S. J.; Park, J. H.; Thorgaard, S. N. In *Nanoelectrochemistry*; Mirkin, M. V., Shigeru, A., Eds.; CRC Press: Boca Raton, FL, 2015; Chapter 8.
(12) Kim, B.-K.; Boika, A.; Kim, J.; Dick, J. E.; Bard, A. J. *J. Am. Chem. Soc.* **2014**, *136*, 4849–4852.
(13) Dick, J. E.; Renault, C.; Kim, B.-K.; Bard, A. J. *Angew. Chem., Int. Ed.* **2014**, *53*, 11859–11862.
(14) Boika, A.; Thorgaard, S. N.; Bard, A. J. *J. Phys. Chem. B* **2013**, *117*, 4371–4380.
(15) Dick, J. E.; Hilterbrand, A. T.; Boika, A.; Upton, J. W.; Bard, A. J. *Proc. Natl. Acad. Sci. U.S.A.* **2015**, *112*, 5303–5308.
(16) Fosdick, S. E.; Anderson, M. J.; Nettleton, E. G.; Crooks, R. M. *J. Am. Chem. Soc.* **2013**, *135*, 5994–5997.

DOI: 10.1021/jacs.5b04545
J. Am. Chem. Soc. 2015, 137, 8376–8379

(17) Kwon, S. J.; Zhou, H.; Fan, F.-R. F.; Vorobyev, V.; Zhang, B.; Bard, A. J. *Phys. Chem. Chem. Phys.* **2011**, *13*, 5394−5402.
(18) See, for example: Kim, J.; Kim, B.-K.; Cho, S.-K.; Bard, A. J. *J. Am. Chem. Soc.* **2014**, *136*, 8173−8176.

DOI: 10.1021/jacs.5b04545
J. Am. Chem. Soc. 2015, 137, 8376−8379